

# Optimization of Coupling Efficiency of Fiber Optic Rotary Joint by Ray Tracing

Chun-Han Chou<sup>a</sup>, Rou-Jhen Chen, Hsin-Yi Tsai<sup>b</sup>, Kuo-Cheng Huang and Chih-Chung Yang  
National Applied Research Laboratories, Taiwan Instrument Research Institute, 20 R&D Rd. VI, Hsinchu Science Park,  
Hsinchu City 30076, Taiwan

**Keywords:** Fiber Optic Rotary Joint, Coupling, Manufacture Error, Dove Prism, Tolerance Analysis.

**Abstract:** In the paper, a misalignment and field magnification tolerance analysis for the coupling efficiency of fiber optic rotary joint was presented. The analysis consisted of output position deviations from different wavelengths, dove prism manufacturing errors, light tilt and decenter errors. It helped manufacturers easily defined component specifications and assembly tolerances for fiber optic rotary joint. The 2 mm spot size was best suited for current assembly tolerances. The 2 mm beam diameter of coupling efficiency was over 80% in the tilt error  $\pm 10$  arcmin and decenter error  $\pm 250$   $\mu\text{m}$ . In the future, we could create a FORJ system according to the simulation parameters. The practice experiment data would compare to our simulation results that used to prove our simulation results.

## 1 INTRODUCTION

Currently, the automation industry was growing rapidly. It required a large number of signal transmission components to connect each part of the component. The fiber optic rotary joint (FORJ) was used to transmit signals across rotary interface (Jia, Jing, Zhang, Wang, Tang and Zhang, 2005). FORJ was widely used in the lot of fields of remotely operated vehicles, oceanographic winches, cable reels, towed arrays, dipping sonar, undersea telemetry and Robotics etc. The traditional multi-pass of FORJ required high precision alignment to reduce signal coupling losses (Liu, Zhu, Jiang and Gao, 2013). Due to manufacturing difficulties, people began to look for another way to solve the problem. People began to use the different ways of C-lens (Jia, Jing, Zhang, Zhou, Zhang and Tang, 2005) and GRIN lens (Shi, Klafter and Harstead, 1985). Even these methods could reduce the coupling loss, but it was difficult to continuously transmit multi-signals when the interface continue rotation. Another group of People used other ways of multi-reflector mirror (Liu and Chen, 2006), diffractive element (Mathias and Sverker, 1999) and symmetrical optical system (DENG, ZHOU and LIU, 2001) etc. These methods could overcome the problem of multiple

signal transmission, but these systems had the disadvantages of large system size and high cost etc. Previously problems were solved until people used dove prism for FORJ. The structure of FROJ composed of fiber array, collimator lens and dove prism. The system was smaller than the multi-mirror and symmetrical optics, and it continued to transmit multiple signals as the interface continued to rotate (Jia, Yu, Jing, Zhang, and Zhang, 2008). The key factor of the dove prism type of FORJ was the manufacture error of dove prism and the assemble tolerance of the system (Shapar, 2018). Enoch group used exact ray trace to calculate the interferometric Dove prism tolerance to manufacturing errors, but they didn't mention the prism alignment tolerance (Gutierrez-Herrera and Strojnik, 2008).

Therefore, we presented a misalignment and field magnification tolerance analysis for the FORJ coupling efficiency. It helped producers easily defined element specifications and assembly tolerances for FORJ. The tolerance analysis had the output position deviation of different wavelength, light source position error, dove prism manufacture error, light source tilt and decenter error. Tolerance analysis showed the complete relationship between coupling efficiency and manufacturing and assembly errors.

<sup>a</sup>  <https://orcid.org/0000-0003-2460-5875>

<sup>b</sup>  <https://orcid.org/0000-0001-8275-6132>

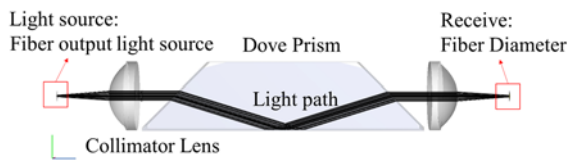


Figure 1: FORJ simulation model.

In the section 2, the FORJ simulation parameters and light propagation mathematical formula were introduced. In the section 3, the tolerance analysis results were introduced. In the section 4, the simulation results are discussed. In the section 5, the conclusion was introduced.

## 2 FORJ MODEL CONSTRUCTION

The FORJ tolerance analysis composed of output position deviation of different wavelength, light source position error, dove prism manufacture error, light source tilt and decenter error. The tolerance analysis was created by the optical simulation software (FRED). The software simulated the propagation of light through FORJ by raytracing. The FORJ composed of fiber, collimation lens and dove prism, as shown in Figure 1.

The light output through the collimating lens was approximately parallel to the optical axis of the dove prism. In the ideal dove model, the direction of light propagation after the dove was the same as the input light. In practice, the dove prism had manufacturing errors, so the direction of the output light was different from the direction of the input light, as shown in Figure 2. In the paper, the size of dove prism was  $25 \times 25 \times 105.68 \text{ mm}^3$  with the size tolerance of  $\pm 0.13$  Legs,  $\pm 0.38$  Hypotenuse. The angular tolerance of the dove prism input and output interface was  $2 \text{ armin}$  [13].

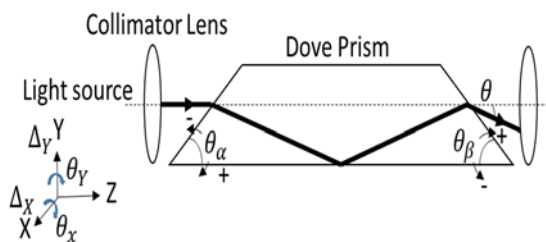


Figure 2: Ray propagation in the dove prism.

The ray propagation output deviation formula:

$$\theta = \theta_\alpha - \cos^{-1}(n \sin[\theta_\alpha - \theta_\beta + \sin^{-1}(\frac{1}{n} \cos \theta_\alpha)]) \quad (1)$$

Where  $\theta_\alpha$  is the input surface of dove prism,  $\theta_\beta$  is the exit surface of dove prism,  $n$  is the dove prism reflection index.

In the optical simulation software, we built a complete FORJ model. These simulated parameters were collected from the actual optical components. Through different dove prism manufacturing errors and assembly errors, we could obtain different efficiency, spot size and spot position on the receiver, as shown in Figure 3. These data could use to create the tolerance analysis.

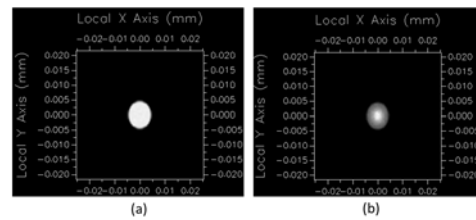


Figure 3: Simulation irradiance map. (a) Fiber output light source. (b) Through the FROJ output light source.

## 3 THE FORJ TOLERANCE ANALYSIS

### 3.1 Output Spot Position of Different Wavelength

The wavelengths commonly used for fiber-optic communication signals were 850 nm, 1310 nm, and 1550 nm. The different wavelength had the different reflection index in the same material. Therefore, different wavelengths of light passing through the dove prism had different spot positions, as shown in Figure 4. The short wavelengths had a higher reflectance index in dove prism materials, so the positional deviation was larger. The positional deviation between 850 nm and 1550 nm was approximately  $400 \mu\text{m}$ . Therefore, the position of receiver of FORJ could tune from 0 to  $400 \mu\text{m}$ , it could accommodate the three different communication wavelengths.

### 3.2 Fiber Couple Tolerance Analysis

The FORJ coupling error consisted of dove prism manufacturing errors, source tilt and decenter errors. The light source generated beams of different diameters through the collimating lens. The beams of different diameters affected the FORJ tolerance distribution. In this section, we used different diameter beams to perform tolerance analysis in

different dove prism manufacturing errors, as shown in Figure 5, 6 & 7.

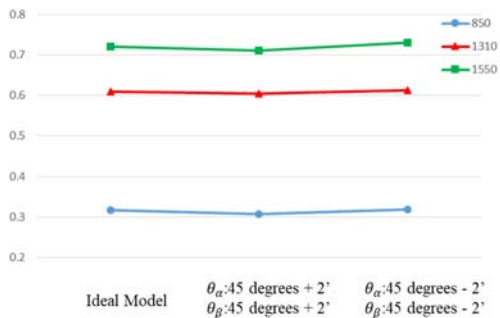


Figure 4: The different manufactory errors of FORJ of output spot position deviation with different wavelength.

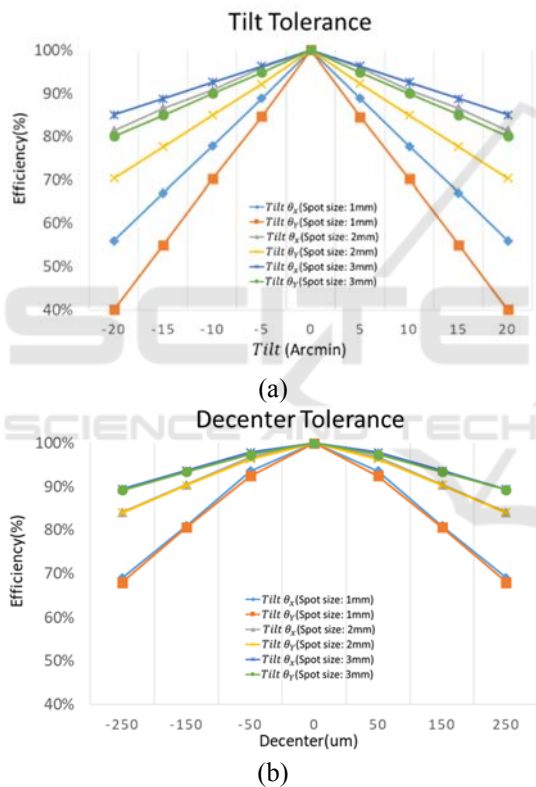


Figure 5: Different diameter beams tolerance analysis in the ideal dove Prism. (a) Input light tilt tolerance analysis. (b) Input light decenter tolerance analysis.

According to the tolerance simulation results, the tolerance distribution of the small diameter beam was more sensitive than the large diameter beam. When the diameter of beam was 1mm and the light of tilt Y tolerance was  $\pm 20$  arcmin, the coupling efficiency dropped to 40%. When the diameter of beam was 3mm and the light of tilt Y tolerance was  $\pm 20$  arcmin, the coupling efficiency was still over 80%. When the

decenter was within  $\pm 250 \mu\text{m}$ , the beam coupling efficiency over 2 mm diameter exceeded 80%. In the manufacturing error of different dove prisms, the tolerance distribution changed, and the efficiency difference was about 5%.

#### 4 DISCUSSION

The spot positional deviation between 850 nm and 1550 nm was approximately  $400 \mu\text{m}$ . The key factor affecting the assembly tolerance distribution was the beam diameter. The tolerance distribution of the tilt Y felled faster than the tilt X. When the diameter of beam was 1mm and the light of tilt Y tolerance was  $\pm 20$  arcmin, the coupling efficiency dropped to 40%. When the diameter of beam was 3 mm and the light of tilt Y tolerance was  $\pm 20$  arcmin, the coupling efficiency was still over 80%. When the decenter was within  $\pm 250 \mu\text{m}$ , the beam coupling efficiency over 2 mm diameter exceeded 80%. Therefore, in the assembly tolerance, the tilt tolerance was more sensitive than the decenter tolerance.

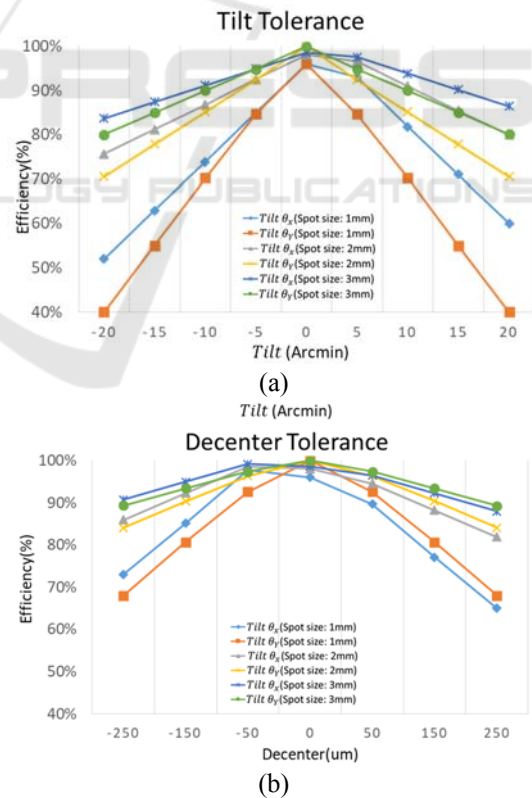


Figure 6: Different diameter beams tolerance analysis in the manufacture error dove Prism. ( $\theta_\alpha: 45^\circ - 2'$ ,  $\theta_\beta: 45^\circ - 2'$ ) (a) Input light tilt tolerance analysis. (b) Input light decenter tolerance analysis.

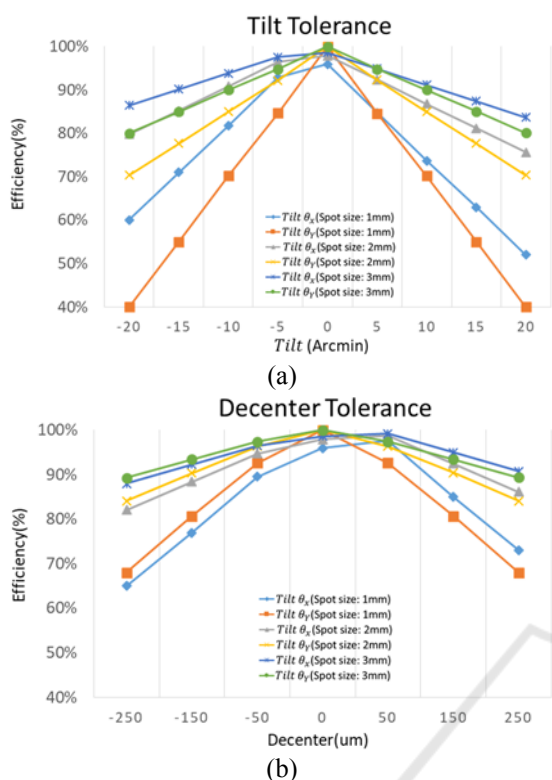


Figure 7: Different diameter beams tolerance analysis in the manufacture error dove Prism. ( $\theta_\alpha$ :45 degrees + 2',  $\theta_\beta$ :45 degrees + 2') (a) Input light tilt tolerance analysis. (b) Input light decenter tolerance analysis.

At present, the optical component tilt error was less than  $\pm 10$  arc minutes, and the decenter error was less than  $\pm 50$   $\mu\text{m}$ . Therefore, in the current assembly tolerances, the suitable beam diameter was 2 mm. The 2 mm beam diameter of coupling efficiency was over 80% in the tilt error  $\pm 10$  arcmin and decenter error  $\pm 250$   $\mu\text{m}$ . The 2 mm cross-sectional area was 44% smaller than the 3 mm cross-sectional area. The FORJ could arrange more fibers and transmit more signals at the same time. If the FORJ want to accommodate three different communication wavelengths, he position of receiver of FORJ required tuning range from 0 to 400  $\mu\text{m}$ .

## 5 CONCLUSIONS

In the paper, a misalignment and field magnification tolerance analysis for the coupling efficiency of FORJ was presented. It helped producers easily define element specifications and assembly tolerances for FORJ. The 2 mm beam diameter was the most suitable for current assembly tolerances. The

coupling efficiency exceeded 80% when the tilt error was  $\pm 10$  arcmin and the decenter error was  $\pm 250$   $\mu\text{m}$ . If the FORJ want to accommodate three different communication wavelengths, the position of receiver of FORJ required tuning range from 0 to 400  $\mu\text{m}$ . In the future, we could create a FORJ system according to the simulation parameters. The practice experiment data would compare to our simulation results that used to prove our simulation results.

## ACKNOWLEDGEMENTS

The authors would like to express their appreciation for financial aid from the Ministry of Science and Technology, R.O.C under grant numbers MOST 108-2221-E-492-019, MOST 108-2218-E-492-010 and MOST 107-2622-E-492-017-CC3. The authors would also like to express their gratitude to the Taiwan Instrument Research Institute of National Applied Research Laboratories for the support.

## REFERENCES

- Jia, D., Jing, W., Zhang, Y., Wang, G., Tang, F., & Zhang, J. (2005). Bidirectional dynamic data transmission through a rotary interface. *Optical Engineering*, 44(5), 050503.
- Liu, J., Zhu, B., Jiang, H., & Gao, W. (2013). Image analysis measurement of cottonseed coat fragments in 100% cotton woven fabric. *Fibers and Polymers*, 14(7), 1208-1214.
- Jia, D. G., Jing, W. C., Zhang, Y. M., Zhou, G., Zhang, J., & Tang, F. (2005). Low-loss fiber optic rotary joint using C-lens collimators. *Optoelectronics Letters*, 1(3), 221.
- Shi, Y., Klafter, L., & Harstead, E. (1985). A dual-fiber optical rotary joint. *Journal of lightwave technology*, 3(5), 999-1004.
- Liu, L., & Chen, N. G. (2006). Double-pass rotary mirror array for fast scanning optical delay line. *Applied optics*, 45(21), 5426-5431.
- Mathias Johansson, Sverker Hard. (1999). Design, fabrication, and evaluation of a multi-channel diffractive optic rotary joint, *Applied Optics*, 38(8): 1302-1310
- Deng, Y. X., Zhou, G., & Liu, W. (2001). Dual-channel fiber optic rotary joint of symmetrical optical system, *Journal of Optoelectronics-Laser*, 12 (8) : 792-794
- Jia, D., Yu, C., Jing, W., Zhang, H., & Zhang, Y. (2008, January). Effect of misalignment on rotating coupling efficiency of the Dove prism. In *Advanced Materials and Devices for Sensing and Imaging III* (Vol. 6829, p. 68290S). International Society for Optics and Photonics.

- Shapar, V. (2018). Principles of compensation of optical rays' rotation and multi-channel optical rotary connectors. *Applied optics*, 57(27), 8023-8033.
- Gutierrez-Herrera, E., & Strojnik, M. (2008). Interferometric tolerance determination for a Dove prism using exact ray trace. *Optics Communications*, 281(5), 897-905.

